Error Control for Molecular Statics Problems

Serge Prudhomme [1], Paul T. Bauman [2], and J. Tinsley Oden [3]

Institute for Computational Engineering and Sciences
The University of Texas at Austin
Austin, Texas 78712

Abstract

In this paper, we present an extension of goal-oriented error estimation and adaptation to the simulation of multi-scale problems of molecular statics. Computable error estimates for the quasicontinuum method are developed with respect to specific quantities of interest and an adaptive strategy based upon these estimates is proposed for error control. The theoretical results are illustrated on a nanoindentation problem in which the quantity of interest is the force acting on the indenter. The promising capability of such error estimates and adaptive procedure for the solution of multi-scale problems is demonstrated on numerical examples.

Key words: Molecular statics, goal-oriented adaptive modeling, error estimation, multi-scale problems, quasicontinuum method.

1 Introduction

Computational methods for the study of multi-scale phenomena have become a prominent area of research in computational science. Indeed, computing capabilities have reached a point where atomistic simulations using quantum mechanical, atomistic potential, and mesoscopic and continuum models can be coupled concurrently to study physical problems of an inherent multi-scale nature [2,8]. Development of such methods is of particular interest for the

Email address: serge@ices.utexas.edu (Serge Prudhomme).
[1] Corresponding author: Research Scientist, ICES.
[2] Graduate Research Assistant and DOE Fellow.
[3] Director of ICES and Cockrell Family Regents Chair of Engineering.

Report Documentation Page

Form Approved
OMB No. 0704-0188

1. REPORT DATE	2. REPORT TYPE	3. DATES COVERED
11 AUG 2005		**00-00-2005 to 00-00-2005**

4. TITLE AND SUBTITLE	5a. CONTRACT NUMBER
Error Control for Molecular Statics Problems	5b. GRANT NUMBER
	5c. PROGRAM ELEMENT NUMBER
6. AUTHOR(S)	5d. PROJECT NUMBER
	5e. TASK NUMBER
	5f. WORK UNIT NUMBER
7. PERFORMING ORGANIZATION NAME(S) AND ADDRESS(ES) **Institute for Computational Engineering and Sciences,The University of Texas at Austin,Austin,TX,78712**	8. PERFORMING ORGANIZATION REPORT NUMBER
9. SPONSORING/MONITORING AGENCY NAME(S) AND ADDRESS(ES)	10. SPONSOR/MONITOR'S ACRONYM(S)
	11. SPONSOR/MONITOR'S REPORT NUMBER(S)

12. DISTRIBUTION/AVAILABILITY STATEMENT
Approved for public release; distribution unlimited

13. SUPPLEMENTARY NOTES
The original document contains color images.

14. ABSTRACT

15. SUBJECT TERMS

16. SECURITY CLASSIFICATION OF:			17. LIMITATION OF ABSTRACT	18. NUMBER OF PAGES	19a. NAME OF RESPONSIBLE PERSON
a. REPORT	b. ABSTRACT	c. THIS PAGE			
unclassified	**unclassified**	**unclassified**		**24**	

study of the mechanics of materials including fracture phenomena, nanoindentation, atomic friction, etc., to name just a few [19,1]. However, many of the existing methods to date, to the best knowledge of the authors, lack some analysis of the error incurred by coupling such models. Furthermore, convergence analysis and comparison studies of these methods seem to be scarce and not fully addressed in the literature. In this paper, we present an application of goal-oriented error estimation and adaptive modeling to a model nanoindentation problem to partially address some of these issues. These ideas draw upon work in [11] where error estimates for quantities of interest are derived. Ideas of goal-oriented adaptive modeling come from [13] and references therein. This goal-oriented modeling methodology has been successfully applied to the study of heterogeneous elastostatics and elastodynamics, random heterogeneous materials, as well as the study of linear lattice models [14,16,12]. See also [13].

In this study, an atomistic model based upon potentials of the embedded-atom method (EAM) is used as a base model to simulate the nanoindentation of a thin aluminum film [4,5]. The target problem was also studied in [19]. Surrogate models are generated using the quasicontinuum method (QCM) [20,18]. Error estimates in a quantity of interest are derived and an adaptive modeling scheme is implemented in the freely available QCM code [10]. A brief summary of some of our results given in this paper were reported in the survey article [13]. Here we give full details of an analysis of multi-scale modeling in which the coarse-scale modeling is implemented using the QCM.

The paper is organized as follows: following the introduction, we present in Section 2 the base model for molecular statics problems, derive a surrogate model based on the quasicontinuum method, and describe a practical example that deals with the nanoindentation of a thin film aluminum crystal. Section 3 is devoted to the derivation of error estimates with respect to quantities of interest. These estimates approximate the modeling error between solutions of the base and surrogate models. In Section 4, an adaptive strategy is proposed for the control of the modeling error by subsequent enrichment of the surrogate model. Performance of the error estimator and adaptive strategy is demonstrated on the nanoindentation problem described in Section 2. We finally give some concluding remarks in Section 5.

2 Molecular statics model

In this section, we consider the problem of determining static equilibrium configurations of a regular lattice of N atoms. The base problem is obtained by minimizing the potential energy of the system consisting of all atoms in

the lattice. In many applications, N can be very large and the base problem is often intractable. In order to reduce its complexity, we consider here the use of an approximation method such as the quasicontinuum method (QCM) [18–20]. In recent years, QCM has become a popular approach for constructing surrogate problems that retain only a small number of active atoms during the simulations. In that sense, QCM can be viewed as a model reduction procedure.

2.1 The base problem. Let $\mathcal{L}$ be a regular lattice of N atoms in $\mathbb{R}^d$, $d = 2$ or 3. The positions of the atoms are given in the reference configuration by the vectors $\hat{\boldsymbol{x}}_i \in \mathbb{R}^d$, $i = 1, \ldots, N$. When the lattice is subjected to a deformation $\boldsymbol{\phi} : \mathbb{R}^d \to \mathbb{R}^d$, the atoms move to the new positions

$$\boldsymbol{x}_i = \boldsymbol{\phi}(\hat{\boldsymbol{x}}_i) = \hat{\boldsymbol{x}}_i + \boldsymbol{u}_i, \quad i = 1, \ldots, N \tag{1}$$

where $\boldsymbol{u}_i$ is the displacement of atom i. We assume that the lattice in the reference configuration covers the region $\bar{\Omega}$, where Ω is an open bounded set of $\mathbb{R}^d$ with boundary $\partial\Omega$. We also assume that the atoms lying on $\partial\Omega$ are all ascribed essential boundary conditions in the form

$$\boldsymbol{u}_i = \boldsymbol{g}_i, \qquad \forall \hat{\boldsymbol{x}}_i \in \partial\Omega \tag{2}$$

with $\boldsymbol{g}_i \in \mathbb{R}^d$. Other boundary conditions will be considered in the nanoindentation application. We deliberately choose to restrict ourselves to this case in the presentation of the theoretical results as, otherwise, it would make the exposition rather cumbersome without adding to the understanding of the methodology. Let N_a be the number of atoms inside the domain Ω and N_b the number of atoms on $\partial\Omega$ such that $N = N_a + N_b$. Henceforth, we shall use the convention that the interior atoms be numbered from 1 to N_a and the boundary atoms from $N_a + 1$ to N. We will consider the finite-dimensional vector spaces $V = (\mathbb{R}^d)^N$ and $V_0 = (\mathbb{R}^d)^{N_a}$. In what follows, we will conveniently use the notation $\boldsymbol{u} = (\boldsymbol{u}_1, \boldsymbol{u}_2, \ldots, \boldsymbol{u}_N)$, $\boldsymbol{u} \in V$, to refer to the displacements of the collection of N atoms. Similarly, $\boldsymbol{u} \in V_0$ is the set of displacements $\boldsymbol{u} = (\boldsymbol{u}_1, \boldsymbol{u}_2, \ldots, \boldsymbol{u}_{N_a})$.

Let a state of the system of N atoms be described by the displacements $\boldsymbol{u} \in V$. The total potential energy of the system is assumed to take the form

$$E(\boldsymbol{u}) = -\sum_{i=1}^{N} \boldsymbol{f}_i \cdot \boldsymbol{u}_i + \sum_{k=1}^{N} E_k(\boldsymbol{u}) \tag{3}$$

where $\boldsymbol{f}_i$ is the external load applied to an atom i and $E_k(\boldsymbol{u})$ is the energy of atom k determined from inter-atomic potentials. Explicit description of E_k will be given below.

The goal of molecular statics is to find the equilibrium state $\boldsymbol{u} \in V$ that minimizes the total potential energy of the system, i.e.

$$E(\boldsymbol{u}) = \inf_{\substack{\boldsymbol{v} \in V \\ \boldsymbol{v}_i = \boldsymbol{g}_i \text{ on } \partial\Omega}} E(\boldsymbol{v}) \tag{4}$$

The constrained minimization problem is then equivalent to finding $\boldsymbol{u} \in V$ such that:

$$\sum_{k=1}^{N} \frac{\partial E_k}{\partial \boldsymbol{u}_i}(\boldsymbol{u}) = \boldsymbol{f}_i, \qquad i = 1, \ldots, N_a \tag{5}$$

$$\boldsymbol{u}_i = \boldsymbol{g}_i, \qquad i = N_a + 1, \ldots, N \tag{6}$$

where $\partial/\partial \boldsymbol{u}_i$ is the gradient vector with respect to each component $u_{l,i}$, $l = 1, \ldots, d$ of the displacement vector $\boldsymbol{u}_i$, i.e. $\partial/\partial \boldsymbol{u}_i = (\partial/\partial u_{1,i}, \ldots, \partial/\partial u_{d,i})$.

A variational formulation of the above problem is obtained by multiplying the N_a equations in (5) by arbitrary vectors $\boldsymbol{v} \in V_0$ so that the problem reads

Find $\boldsymbol{u} \in V$ *such that*

$$\begin{aligned} B(\boldsymbol{u}; \boldsymbol{v}) &= F(\boldsymbol{v}), \quad \forall \boldsymbol{v} \in V_0 \\ \boldsymbol{u}_i &= \boldsymbol{g}_i, \quad i = N_a + 1, \ldots, N \end{aligned} \tag{7}$$

where the semilinear form $B(\cdot;\cdot)$ and linear form $F(\cdot)$ are defined for any $\boldsymbol{u} \in V$ and $\boldsymbol{v} \in V_0$ as

$$\begin{aligned} B(\boldsymbol{u}; \boldsymbol{v}) &= \sum_{i=1}^{N_a} \left[\sum_{k=1}^{N} \frac{\partial E_k}{\partial \boldsymbol{u}_i}(\boldsymbol{u}) \right] \cdot \boldsymbol{v}_i \\ F(\boldsymbol{v}) &= \sum_{i=1}^{N_a} \boldsymbol{f}_i \cdot \boldsymbol{v}_i \end{aligned} \tag{8}$$

Note that Problem (7) is nonlinear in $\boldsymbol{u}$ and linear in $\boldsymbol{v}$. We assume that there exist solutions and that it can be solved by a quasi-Newton method (see [17] for details).

2.2 The surrogate problem by the quasicontinuum method. We describe in this section the main features of QCM. The reader is referred to [18,17,9] for a detailed exposition. The objectives of the method can be summarized as follows: (i) to dramatically reduce the number of degrees of freedom from $N \times d$, and (ii) to substantially reduce the cost in the calculation of the potential energy by computing energies only at selected sites. In addition, the use of

adaptive approaches for automatic selection of the degrees of freedom can allow QCM to capture the critical deformations of the lattice in an efficient manner.

The initial step of the method consists in choosing a set of $R \ll N$ representative atoms, the so-called "repatoms", and in approximating $\boldsymbol{u} \in V$ by the reduced vector $\boldsymbol{u}_0 \in W = (\mathbb{R}^d)^R$. The displacements $\boldsymbol{u}_0$ represent the active degrees of freedom of the system and the repatoms are conveniently identified with the nodes of a finite element triangulation $\mathcal{P}_h$ of Ω. The displacements of the $(N - R)$ "slave" atoms are then interpolated from $\boldsymbol{u}_0$ by piecewise linear polynomials defined on the triangular mesh. Let ϕ_r, $r = 1, \ldots, R$, denote the basis functions (the hat functions) associated with $\mathcal{P}_h$ and let $\boldsymbol{u}_h$ be the finite element vector function such that

$$\boldsymbol{u}_h(\hat{\boldsymbol{x}}) = \sum_{r=1}^{R} \boldsymbol{u}_{0,r} \phi_r(\hat{\boldsymbol{x}}), \qquad \forall \hat{\boldsymbol{x}} \in \bar{\Omega} \tag{9}$$

$\boldsymbol{u}_0 = (\boldsymbol{u}_{0,1}, \boldsymbol{u}_{0,2}, \ldots, \boldsymbol{u}_{0,R}) \in W$. The displacements of the N atoms in the lattice can clearly be evaluated from $\boldsymbol{u}_0$ as

$$\boldsymbol{u}_i^0 = \boldsymbol{u}_h(\hat{\boldsymbol{x}}_i), \qquad i = 1, \ldots, N \tag{10}$$

so that $\boldsymbol{u}^0 = (\boldsymbol{u}_1^0, \boldsymbol{u}_2^0, \ldots, \boldsymbol{u}_N^0) \in V$. This extension operator will be referred to as $\boldsymbol{\pi} : W \to V$ such that $\boldsymbol{\pi}\boldsymbol{u}_0 = \boldsymbol{u}^0$. In a similar manner, defining R_a and R_b as the number of repatoms lying in the interior of the lattice and on the boundary $\partial\Omega$, respectively, and letting $W_0 = (\mathbb{R}^d)^{R_a}$, we also introduce the extension operator $\boldsymbol{\pi}_0 : W_0 \to V_0$. The reduced vector $\boldsymbol{\pi}\boldsymbol{u}_0$ could be used to approximate the total potential energy

$$E(\boldsymbol{\pi}\boldsymbol{u}_0) = -\sum_{i=1}^{N} \boldsymbol{f}_i \cdot (\boldsymbol{\pi}\boldsymbol{u}_0)_i + \sum_{k=1}^{N} E_k(\boldsymbol{\pi}\boldsymbol{u}_0) \tag{11}$$

but such a calculation would still be very prohibitive as all N atoms need to be visited in order to sum up the atomic site energies.

The second step of the QCM is thus concerned with and efficient scheme to approximate the total energy $E(\boldsymbol{\pi}\boldsymbol{u}_0)$. The main motivation here is to estimate the potential energy by summing only over the repatoms such that

$$E(\boldsymbol{\pi}\boldsymbol{u}_0) \approx E_0(\boldsymbol{u}_0) = -\sum_{r=1}^{R} n_r \, \boldsymbol{f}_{0,r} \cdot \boldsymbol{u}_{0,r} + \sum_{r=1}^{R} n_r E_r(\boldsymbol{u}_0) \tag{12}$$

where n_r is an appropriate weight function associated with repatom r so as to account for all atoms in the lattice, i.e. $\sum_r n_r = N$, and $\boldsymbol{f}_{0,r}$ is the averaged

external force acting on repatom r. In the QCM, the calculation of the energies $n_r E_r(\boldsymbol{u}_0)$ is done in one of two ways, depending upon whether a repatom is considered either "local" or "nonlocal". The attribute "local" refers here to the fact that the energy at a point in the continuum depends on the deformation at that point only and not on its surroundings. Let R_{lc} denote the number of local repatoms and R_{nl} the number of nonlocal repatoms, $R = R_{lc} + R_{nl}$. The atomistic energies are now separated into local and nonlocal contributions such as:

$$\sum_{r=1}^{R} n_r E_r(\boldsymbol{u}_0) = \sum_{r=1}^{R_{lc}} n_r E_r^{loc}(\boldsymbol{u}_0) + \sum_{s=1}^{R_{nl}} n_s E_s^{nl}(\boldsymbol{u}_0) \tag{13}$$

Note that if $R_{nl} = 0$, the method is called the *local QCM*, and if $R_{lc} = 0$, the *nonlocal QCM*. Otherwise, the method is referred to as the *coupled local/nonlocal QCM*. We shall only consider the latter in what follows.

Local formulation: The local formulation makes use of the Cauchy-Born rule [7] to compute the sites energies. The Cauchy-Born rule postulates that when a crystal is subjected to a small linear displacement of its boundary, then all interior atoms are deformed following this displacement. In particular, this means that every atom in a region experiencing a uniform deformation gradient has the same energy. Since the QCM uses piecewise linear finite elements, the deformation gradient is uniform within each element and the energy in an element can be calculated by computing the energy of one atom only in the deformed state. Then the energy E_r^{loc} is given by:

$$n_r E_r^{loc}(\boldsymbol{u}_0) = \sum_{e=1}^{K} n_r^e \, \mathcal{E}(\boldsymbol{F}_e), \qquad n_r = \sum_{e=1}^{K} n_r^e \tag{14}$$

where $\mathcal{E}(\boldsymbol{F}_e)$ is the energy of a single atom under the deformation gradient $\boldsymbol{F}_e$. Here K is the number of elements surrounding the repatom r and n_r^e is the number of atoms from n_r that actually live in element e.

Nonlocal formulation: In this formulation, the energy is accurately approximated by explicitly computing the energy of the nonlocal repatoms, i.e. $E_s^{nl}(\boldsymbol{u}_0) = E_s(\boldsymbol{u}_0)$. In other words, if $R_{lc} = 0$ and in the limit case where every atom in the lattice is made a repatom, that is $R_{nl} = N$, then $n_r = 1$, $r = 1, \ldots, N$, and the problem becomes equivalent to the base problem.

Remark 1 ***(Ghost forces)*** *The coupling of nonlocal and local representative atoms leads to spurious forces, so-called "ghost forces", near interfaces of local and nonlocal repatoms. The issue is that the energy calculated at a nonlocal repatom may be influenced by the displacement of a local repatom nearby, while the converse may not be true. Therefore the approximation of the energy by the coupled local/nonlocal approach yields non-physical forces at the interface*

of the local and nonlocal regions. A solution to this issue has been devised by adding corrective forces to balance ghost forces (see e.g. [17]).

Remark 2 ***(Local/nonlocal criterion)*** *The selection of representative atoms as local or nonlocal is based upon the variation of the deformation gradient on the atomic scale in the vicinity of the atoms. A repatom is made local if the deformation is almost uniform, nonlocal if the deformation gradient is large. In the QCM, the deformation gradients are compared element to element by computing the differences between the eigenvalues of the right stretch tensor* $\boldsymbol{U} = \sqrt{\boldsymbol{F}^T \boldsymbol{F}}$ *in each element,* $\boldsymbol{F} = \nabla \boldsymbol{\phi}$ *being the deformation gradient in the elements.*

Using the approximation (12) for the potential energy, the minimization problem for the QCM consists of finding $\boldsymbol{u}_0 \in W$ such that

$$E_0(\boldsymbol{u}_0) = \min_{\substack{\boldsymbol{v} \in W \\ \boldsymbol{v}_i = \boldsymbol{g}_i \text{ on } \partial\Omega}} E_0(\boldsymbol{v}) \tag{15}$$

This can be rewritten in variational form as

$$\begin{aligned} &\textit{Find } \boldsymbol{u}_0 \in W \textit{ such that} \\ &\qquad B_0(\boldsymbol{u}_0; \boldsymbol{v}) = F_0(\boldsymbol{v}), \qquad \forall \boldsymbol{v} \in W_0 \\ &\qquad\qquad \boldsymbol{u}_{0,i} = \boldsymbol{g}_i, \qquad i = R_a + 1, \ldots, R \end{aligned} \tag{16}$$

where the semilinear form $B_0(\cdot;\cdot)$ and linear form $F_0(\cdot)$ are now given by

$$\begin{aligned} B_0(\boldsymbol{u}; \boldsymbol{v}) &= \sum_{i=1}^{R_a} \left[\sum_{r=1}^{R} n_r \frac{\partial E_r}{\partial \boldsymbol{u}_i}(\boldsymbol{u}) \right] \cdot \boldsymbol{v}_i \\ F_0(\boldsymbol{v}) &= \sum_{i=1}^{R_a} n_i \ \boldsymbol{f}_{0,i} \cdot \boldsymbol{v}_i \end{aligned} \tag{17}$$

Remark 3 ***(Adaptivity)*** *In [9], it is proposed that an automatic mesh adaption technique be used to add and remove representative atoms "on the fly", in order to capture the fine features during the simulation. The criterion for adaptivity is based upon the derivation of an error indicator similar to that of Zienkiewicz and Zhu [21] for the finite element method. The error indicator is calculated over each element* Ω_e *as*

$$\eta_K = \sqrt{\frac{1}{|\Omega_K|} \int_{\Omega_K} (\bar{\boldsymbol{F}} - \boldsymbol{F}) : (\bar{\boldsymbol{F}} - \boldsymbol{F}) dx}$$

where $|\Omega_K|$ *is the volume of element* K, $\boldsymbol{F}(\boldsymbol{u}_0)$ *the deformation gradient obtained from the QC solution* $\boldsymbol{u}_0$ *(piecewise constant), and* $\bar{\boldsymbol{F}}$ *is a recovered*

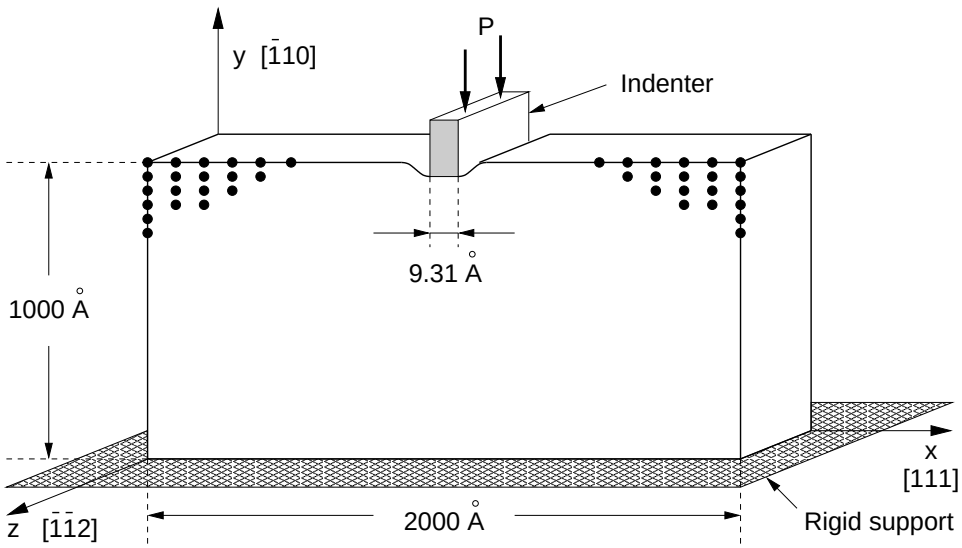

Fig. 1. Nanoindentation of an aluminum crystal.

smooth deformation gradient obtained by a L_2-projection of $\boldsymbol{F}(\boldsymbol{u}_0)$ onto the finite element space (piecewise linear). In the adaptive strategy, the elements that exceed a prescribed tolerance are marked for refinement. This adaptive strategy will be used as is to compute the solution $\boldsymbol{u}_0$ and the "overkill" solution of the problem. Our goal here is to propose an alternative method that automatically adapts the solution process by controlling errors in quantities of interest.

2.3 An application example. Numerical simulations to illustrate the performance of the error estimator and adaptive strategy will be performed on the nanoindentation problem suggested by Tadmor *et al.* [15,17,19]. This example is actually provided as a model example accompanying the open source software package [10].

In this example, a thin film of aluminum crystal is indented by a rigid rectangular indenter, infinite in the out-of-plane direction, as depicted in Fig. 1. The dimensions for the block of crystal are 2000×1000 A^2 (A=Angström) in the [111] and [$\bar{1}$10] directions of the crystal. The crystal rests on a rigid support so that homogeneous boundary conditions $\boldsymbol{u}_i = \boldsymbol{0}$ are prescribed for those atoms i located at $y = 0$. The remaining boundary conditions are enforced as follows: at $x = 0$ and $x = 2000$, homogeneous essential boundary conditions are prescribed in the x- and z-direction while zero forces are prescribed in the y-direction; these boundary conditions enforce symmetry across the planes. The atoms in the $y = 1000$ plane (excluding the atoms under the indenter) are prescribed zero forces. The indenter is moved downward by a succession

of increments $\delta l = 0.2$ A so that the boundary conditions for the atoms i just below the indenter are given by:

$$\boldsymbol{u}_i = (0, -s\,\delta l, 0), \qquad s = 1, \ldots, 30 \tag{18}$$

Quasistatic steps are then considered to solve for the displacements.

The site energies $E_k(\boldsymbol{u})$ of each atom k of the aluminum crystal are modeled by the Embedded Atom Method (EAM), see e.g. [4,6]. Briefly, the semi-empirical potential energy for atom k is given by

$$E_k(\boldsymbol{u}) = F_k(\bar{\rho}_k) - E_k^{(2)}(\boldsymbol{u}), \tag{19}$$

where F_k is interpreted as an electron-density dependent embedding energy, $\bar{\rho}_k$ is an averaged electron density at the position of atom k, and

$$E_k^{(2)}(\boldsymbol{u}) = \frac{1}{2}\sum_{k \neq j} V_{kj}^{(2)}(r_{kj}). \tag{20}$$

Here $V_{kj}^{(2)}$ is a pairwise potential between atoms k and j and r_{kj} denotes the interatomic distance

$$r_{kj} = \sqrt{((\hat{\boldsymbol{x}}_k - \hat{\boldsymbol{x}}_j) + (\boldsymbol{u}_k - \boldsymbol{u}_j)) \cdot ((\hat{\boldsymbol{x}}_k - \hat{\boldsymbol{x}}_j) + (\boldsymbol{u}_k - \boldsymbol{u}_j))} \tag{21}$$

Remark 4 ***(Cutoff functions)*** *The quasicontinuum method employs a cut-off function to approximate the interatomic potentials $V_{kj}^{(2)}$. Since the potential decays rapidly with respect to the interatomic distance r_{kj}, the potential only includes atoms that lie within some short distance between each other.*

The interatomic distances in the undeformed configuration of the crystal are 2.33 A in the x-direction. One $(\bar{1}, \bar{1}, 0)$ layer of the film contains about 1.3 million atoms [19]. Note that the lattice is two-dimensional, but that displacements are allowed in three dimensions (constrained by periodicity in the z-direction) and the energy is calculated based upon three-dimensional displacements.

Rather than solving for the solution of the full base problem (7), an "overkill" solution of the surrogate problem (16) is considered as the reference solution. This solution hereafter will be referred to as the base model solution. This base model solution involves a sufficiently high number of degrees of freedom so that it is considered, for the purposes of this study, a highly accurate approximation of $\boldsymbol{u}$.

The refinement tolerances were set to 0.000075 for the base model solution and to 0.075 for the QC solution (this value is recommended by the authors [10]).

The meshes corresponding to these solutions are shown in Fig. 2. The vertical displacements, at an early stage of the indentation process, and just before dislocation nucleation, are shown in Figs. 3 and 4, respectively. In the early stages, it appears that the displacements computed by the QC solution compare well with the base model solution. However, at the dislocation nucleation, the latter appears to be softer, allowing the slip plane to move more quickly into the material.

For better comparison, we show in Fig. 5 the magnitude of the force exerted by the crystal onto the indenter. This force represents a quantity of physical interest as it clearly indicates the nucleation of the dislocation. Note that the base model solution has been run only to load step 27 due to computational cost. However, the QC solution has been displayed for the full 30 steps. The QC solution seems to be stiffer, causing the dislocations to nucleate one load step sooner than the base model solution as the critical force is reached more quickly. Thus, although the displacements seem to compare well in the linear region, small errors accumulate resulting in an inaccurate portrayal of the mechanics of the lattice. Our goal in the next sections will be to establish estimates of the error in the quasicontinuum solution with respect to this quantity of interest and to control that error via an adaptive algorithm.

3 Error estimation

3.1 Errors and quantity of interest. The errors in the QC solution $\boldsymbol{u}_0$, with respect to the solution of the base problem, arise from three sources: (i) use of an iterative method to solve the nonlinear problem, (ii) reduction of the number of degrees of freedom from N to R, and (iii) approximation of the total potential energy by E_0, as defined in (12) and (13).

The error due to the nonlinear solver is controlled at each iteration and is assumed to be negligible compared to the other sources of error. This error is sometimes referred to as the *solution error*. The second type of error is analogous to *discretization error* in Galerkin approximations such as in the finite element method. Here it can be regarded as a model reduction error. Finally, the last source induces a so-called *modeling error* due to the modeling of the energy using the coupled local/nonlocal QCM. In this work, we will not differentiate the three types of errors and will provide for estimates of the total error.

The next issue when dealing with *a posteriori* error estimation is the selection of the error measure. Early works on the subject have concentrated on global norms such as energy norms. More recently, methods have been developed

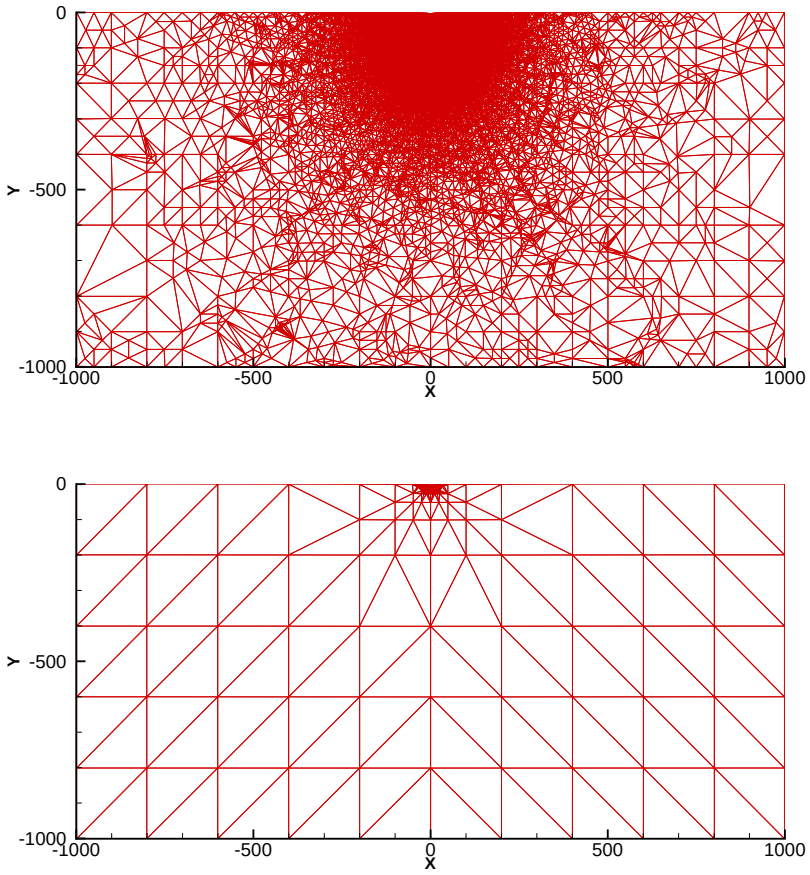

Fig. 2. Finite element triangulation for the base model solution (top) and the QC solution (bottom) at load step 15. The base model solution has 25484 atoms while the QC solution has 445 atoms.

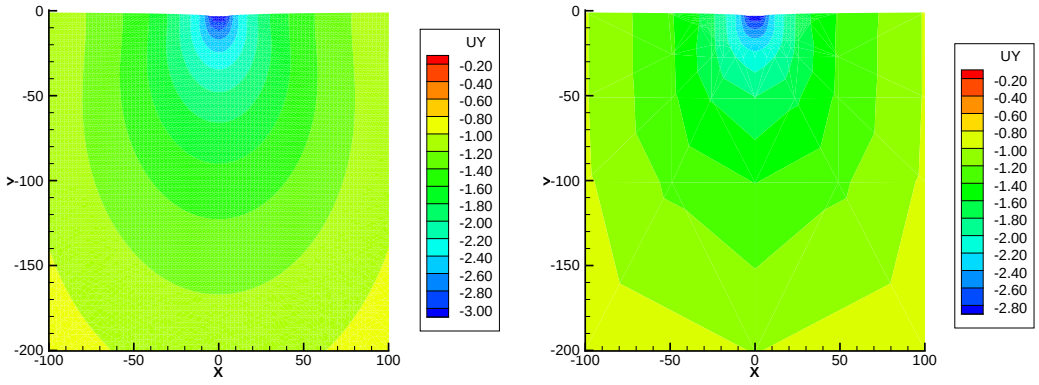

Fig. 3. The base model solution (left) and the QC solution (right) at load step 15.

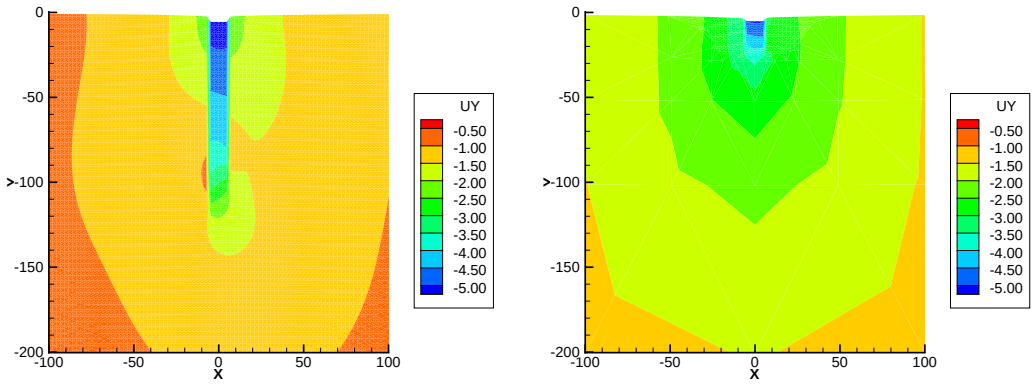

Fig. 4. The base model solution (left) and the QC solution (right) at the beginning of load step 27 and 26, respectively. The base model solution has 40554 atoms while the QC solution has 492 atoms.

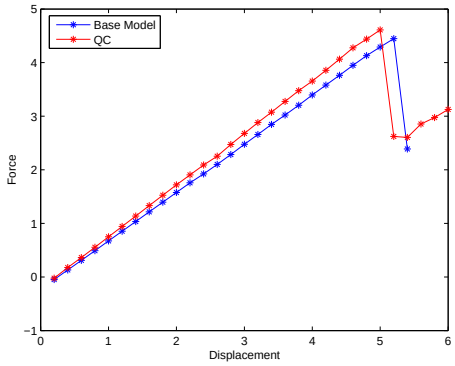

Fig. 5. The force-displacement curve comparing the evolution of the base model solution and the QC solution.

to construct error estimates with respect to quantities of physical interest. A typical quantity of interest in the nanoindentation problem (see Section 2.3) is the reaction force on the indenter. We choose here this force as the quantity of interest for determining error estimates. Let the atoms in contact with the lower surface of the indenter be numbered from 1 to M. Then the force can be written as:

$$Q(\boldsymbol{u}) = -\sum_{i=1}^{M} \boldsymbol{f}_i \cdot \boldsymbol{n} \tag{22}$$

where $\boldsymbol{n}$ is the outward unit normal vector to $\partial\Omega$ below the indenter. In terms of the potential energies, we have:

$$Q(\boldsymbol{u}) = -\sum_{i=1}^{M} \frac{\partial E_i}{\partial \boldsymbol{u}_i}(\boldsymbol{u}) \cdot \boldsymbol{n} \tag{23}$$

We note that $Q(\boldsymbol{u})$ is a nonlinear functional defined on the solution space V. We also assume in the following that the meshes are constructed in such a way that the M atoms under the indenter are representative atoms, and all the forces are computed by the nonlocal approach.

The objective is then to estimate the error quantity

$$\mathcal{E} = Q(\boldsymbol{u}) - Q(\boldsymbol{\pi u}_0) \tag{24}$$

where $\boldsymbol{\pi u}_0 \in V$ is obtained from $\boldsymbol{u}_0$ by (10). To that end, we follow the approach described in [11] and present the dual problem of the base model in the next section.

3.2 The dual problem and error representation. The general approach to obtain estimates of the error $\mathcal{E}$ makes use of the solution of the dual problem associated with the base model (7):

$$\begin{aligned} &\textit{Find } \boldsymbol{p} \in V_0 \textit{ such that} \\ &\qquad B'(\boldsymbol{u}; \boldsymbol{v}, \boldsymbol{p}) = Q'(\boldsymbol{u}; \boldsymbol{v}), \qquad \forall \boldsymbol{v} \in V_0 \end{aligned} \tag{25}$$

where the derivatives are defined as

$$\begin{aligned} B'(\boldsymbol{u}; \boldsymbol{v}, \boldsymbol{p}) &= \lim_{\theta \to 0} \frac{1}{\theta} \left[B(\boldsymbol{u} + \theta \boldsymbol{v}; \boldsymbol{p}) - B(\boldsymbol{u}; \boldsymbol{p}) \right] \\ Q'(\boldsymbol{u}; \boldsymbol{v}) &= \lim_{\theta \to 0} \frac{1}{\theta} \left[Q(\boldsymbol{u} + \theta \boldsymbol{v}) - Q(\boldsymbol{u}) \right] \end{aligned} \tag{26}$$

In the molecular statics case, we have

$$\begin{aligned} B'(\boldsymbol{u}; \boldsymbol{v}, \boldsymbol{p}) &= \sum_{j=1}^{N_a} \sum_{i=1}^{N_a} \boldsymbol{v}_j \cdot \left[\sum_{k=1}^{N} \frac{\partial^2 E_k}{\partial \boldsymbol{u}_j \partial \boldsymbol{u}_i}(\boldsymbol{u}) \right] \cdot \boldsymbol{p}_i \\ Q'(\boldsymbol{u}; \boldsymbol{v}) &= -\sum_{j=1}^{N_a} \boldsymbol{v}_j \cdot \left[\sum_{i=1}^{M} \frac{\partial^2 E_i}{\partial \boldsymbol{u}_j \partial \boldsymbol{u}_i}(\boldsymbol{u}) \cdot \boldsymbol{n} \right] \end{aligned} \tag{27}$$

However, since the dual solution depends on the exact solution $\boldsymbol{u}$ and that the above problem may be intractable due to the large number of atoms, we may use instead approximations of $\boldsymbol{p}$. An approximation can be obtained by solving the surrogate dual problem:

$$\begin{aligned} &\textit{Find } \boldsymbol{p}_0 \in W_0 \textit{ such that} \\ &\qquad B_0'(\boldsymbol{u}_0; \boldsymbol{v}, \boldsymbol{p}_0) = Q_0'(\boldsymbol{u}_0; \boldsymbol{v}), \qquad \forall \boldsymbol{v} \in W_0 \end{aligned} \tag{28}$$

and by extending $\boldsymbol{p}_0$ to the space V_0 to obtain the vector $\boldsymbol{\pi}_0\boldsymbol{p}_0 \in V_0$,

$$\boldsymbol{\pi}_0\boldsymbol{p}_{0,i} = \sum_{r=1}^{R} \boldsymbol{p}_{0,r}\phi_r(\hat{\boldsymbol{x}}_i), \qquad i = 1, \ldots, N \tag{29}$$

The quantity of interest Q_0 in (28) is defined for $\boldsymbol{v} \in W$ by $Q_0(\boldsymbol{v}) = Q(\boldsymbol{\pi}\boldsymbol{v})$.

In the following, we denote by $\boldsymbol{e}_0$ and $\boldsymbol{\varepsilon}_0$ the errors in $\boldsymbol{\pi}\boldsymbol{u}_0$ and $\boldsymbol{\pi}_0\boldsymbol{p}_0$, i.e.

$$\begin{aligned} \boldsymbol{e}_0 &= \boldsymbol{u} - \boldsymbol{\pi}\boldsymbol{u}_0 \in V \\ \boldsymbol{\varepsilon}_0 &= \boldsymbol{p} - \boldsymbol{\pi}_0\boldsymbol{p}_0 \in V_0 \end{aligned} \tag{30}$$

We apply the results of [11] to derive the following theorem that provides for a representation of the error in the quantity of interest:

Theorem 1 *Let the semilinear form $B(\cdot;\cdot)$ in (7) belong to $C^3(V)$ and let the quantity of interest $Q(\cdot)$ as defined in (23) be in $C^3(V)$. Let $\boldsymbol{u} \in V$ and $\boldsymbol{p} \in V_0$ be solutions of the base problems (7) and (25), respectively. Let $(\boldsymbol{u}_0, \boldsymbol{p}_0) \in W \times W_0$ be the solution pair of the surrogate problems and let $(\boldsymbol{\pi}\boldsymbol{u}_0, \boldsymbol{\pi}_0\boldsymbol{p}_0)$ denote their extensions to the spaces $V \times V_0$. Then the error in $Q(\boldsymbol{u})$ produced by $\boldsymbol{\pi}\boldsymbol{u}_0$ is given by*

$$\mathcal{E} = Q(\boldsymbol{u}) - Q(\boldsymbol{\pi}\boldsymbol{u}_0) = \mathcal{R}(\boldsymbol{\pi}\boldsymbol{u}_0; \boldsymbol{p}) + \Delta(\boldsymbol{\pi}\boldsymbol{u}_0, \boldsymbol{\pi}_0\boldsymbol{p}_0, \boldsymbol{e}_0, \boldsymbol{\varepsilon}_0) \tag{31}$$

where $\mathcal{R}(\boldsymbol{\pi}\boldsymbol{u}_0; \boldsymbol{v})$ is the residual functional,

$$\mathcal{R}(\boldsymbol{\pi}\boldsymbol{u}_0; \boldsymbol{v}) = F(\boldsymbol{v}) - B(\boldsymbol{\pi}\boldsymbol{u}_0; \boldsymbol{v}), \quad \boldsymbol{v} \in V_0 \tag{32}$$

and $\Delta = \Delta(\boldsymbol{\pi}\boldsymbol{u}_0, \boldsymbol{\pi}_0\boldsymbol{p}_0, \boldsymbol{e}_0, \boldsymbol{\varepsilon}_0)$ is the remainder,

$$\begin{aligned} \Delta = \frac{1}{2}\int_0^1 \{&B''(\boldsymbol{\pi}\boldsymbol{u}_0 + s\boldsymbol{e}_0; \boldsymbol{e}_0, \boldsymbol{e}_0, \boldsymbol{\pi}_0\boldsymbol{p}_0 + s\boldsymbol{\varepsilon}_0) \\ &- Q''(\boldsymbol{\pi}\boldsymbol{u}_0 + s\boldsymbol{e}_0; \boldsymbol{e}_0, \boldsymbol{e}_0)\} ds \\ + \frac{1}{2}\int_0^1 \{&Q'''(\boldsymbol{\pi}\boldsymbol{u}_0 + s\boldsymbol{e}_0; \boldsymbol{e}_0, \boldsymbol{e}_0) - 3B''(\boldsymbol{\pi}\boldsymbol{u}_0 + s\boldsymbol{e}_0; \boldsymbol{e}_0, \boldsymbol{e}_0, \boldsymbol{\varepsilon}_0) \\ &- B'''(\boldsymbol{\pi}\boldsymbol{u}_0 + s\boldsymbol{e}_0; \boldsymbol{e}_0, \boldsymbol{e}_0, \boldsymbol{e}_0, \boldsymbol{\pi}_0\boldsymbol{p}_0 + s\boldsymbol{\varepsilon}_0)\}(s-1) s ds \end{aligned} \tag{33}$$

Goal-oriented error estimators aim at estimating $\mathcal{E}$ by accurately approximating the quantity $\mathcal{R}(\boldsymbol{\pi}\boldsymbol{u}_0; \boldsymbol{p})$ and neglecting the higher-order terms Δ. One such approach is proposed in the next section.

3.3 The error estimator. We first rewrite the quantity $\mathcal{R}(\boldsymbol{\pi}\boldsymbol{u}_0; \boldsymbol{p})$ in different forms in order to lay down our motivations for the derivation of the error

estimator. Starting from the definition of the residual, it is clear that:

$$\begin{aligned}\mathcal{R}(\boldsymbol{\pi u}_0;\boldsymbol{p}) &= F(\boldsymbol{\pi u}_0,\boldsymbol{p}) - B(\boldsymbol{\pi u}_0;\boldsymbol{p}) \\ &= \sum_{i=1}^{N_a} \boldsymbol{f}_i \cdot \boldsymbol{p}_i - \sum_{i=1}^{N_a}\left[\sum_{k=1}^{N} \frac{\partial E_k}{\partial \boldsymbol{u}_i}(\boldsymbol{\pi u}_0)\right]\cdot \boldsymbol{p}_i \\ &= \sum_{i=1}^{N_a}\left(\boldsymbol{f}_i - \left[\sum_{k=1}^{N} \frac{\partial E_k}{\partial \boldsymbol{u}_i}(\boldsymbol{\pi u}_0)\right]\right)\cdot \boldsymbol{p}_i \\ &= \sum_{i=1}^{N_a} \boldsymbol{r}_i(\boldsymbol{\pi u}_0)\cdot \boldsymbol{p}_i\end{aligned} \tag{34}$$

where the residual vector $\boldsymbol{r}(\boldsymbol{\pi u}_0) \in V_0$ indicates how the forces acting on each atom i fail to be equilibrated. We observe that the calculation of $\mathcal{R}(\boldsymbol{\pi u}_0;\boldsymbol{p})$ may be cost prohibitive when the number of atoms N, or rather N_a, is large. In an effort to reduce the computational cost of the error estimator, it is desirable to take into account only those contributions that are the most significant, meaning that the number of atoms to be considered for the calculation of (34) should range from R_a to N_a.

Moreover, thanks to the linearity of the residual functional, the quantity $\mathcal{R}(\boldsymbol{\pi u}_0;\boldsymbol{p})$ can be decomposed as:

$$\mathcal{R}(\boldsymbol{\pi u}_0;\boldsymbol{p}) = \mathcal{R}(\boldsymbol{\pi u}_0;\boldsymbol{\pi}_0\boldsymbol{p}_0) + \mathcal{R}(\boldsymbol{\pi u}_0;\boldsymbol{\varepsilon}_0) \tag{35}$$

It is well known that the contribution $\mathcal{R}(\boldsymbol{\pi u}_0;\boldsymbol{\pi}_0\boldsymbol{p}_0)$ vanishes for Galerkin approximations. In a similar manner here, this term fails to detect the model reduction error. It follows that the solution $\boldsymbol{p}_0$ provides for a poor approximation of the dual solution $\boldsymbol{p}$, in the sense that $\mathcal{R}(\boldsymbol{\pi u}_0;\boldsymbol{\pi}_0\boldsymbol{p}_0)$ approximates $\mathcal{R}(\boldsymbol{\pi u}_0;\boldsymbol{p})$ poorly, and a better approximation should be obtained in a space larger than W_0.

We propose here to evaluate the residual and the dual solution on a mesh which is finer than the mesh used for the evaluation of $\boldsymbol{u}_0$, but much coarser than the mesh that would be obtained by considering all atoms as representive atoms. Let $\tilde{\mathcal{P}}_h$ denote such a partition of $\bar{\Omega}$ (we shall explain below how to construct $\tilde{\mathcal{P}}_h$) and suppose that it contains a total number of $\tilde{N}$ nodes with $\tilde{N}_a$ interior nodes. We introduce the vector spaces $\tilde{V} = (\mathbb{R}^d)^{\tilde{N}}$ and $\tilde{V}_0 = (\mathbb{R}^d)^{\tilde{N}_a}$ as well as the extension operators $\tilde{\boldsymbol{\pi}} : V \to \tilde{V}$ and $\tilde{\boldsymbol{\pi}}_0 : V_0 \to \tilde{V}_0$. We can now define a residual functional $\tilde{\mathcal{R}}$ on $\tilde{V}$ such that for any $\tilde{\boldsymbol{u}} \in \tilde{V}$ and $\tilde{\boldsymbol{v}} \in \tilde{V}_0$

$$\tilde{\mathcal{R}}(\tilde{\boldsymbol{u}};\tilde{\boldsymbol{v}}) = \sum_{i=1}^{\tilde{N}_a} \tilde{\boldsymbol{r}}_i(\tilde{\boldsymbol{u}})\cdot \tilde{\boldsymbol{v}}_i \tag{36}$$

where the $\tilde{\boldsymbol{r}}_i(\tilde{\boldsymbol{u}})$ are computed via the coupled local/nonlocal quasicontinuum

approach. We will also consider the approximate dual problem:

$$\begin{aligned} &\textit{Find } \tilde{\boldsymbol{p}} \in \tilde{V}_0 \textit{ such that} \\ &\qquad \tilde{B}'(\tilde{\boldsymbol{\pi}}\boldsymbol{u}_0; \tilde{\boldsymbol{v}}, \tilde{\boldsymbol{p}}) = \tilde{Q}'(\tilde{\boldsymbol{\pi}}\boldsymbol{u}_0; \tilde{\boldsymbol{v}}), \qquad \forall \tilde{\boldsymbol{v}} \in \tilde{V}_0 \end{aligned} \tag{37}$$

with, for all $\tilde{\boldsymbol{u}} \in \tilde{V}$ and $\tilde{\boldsymbol{v}} \in \tilde{V}_0$,

$$\begin{aligned} \tilde{B}(\tilde{\boldsymbol{u}}; \tilde{\boldsymbol{v}}) &= \sum_{i=1}^{\tilde{N}_a} \left[\sum_{k=1}^{\tilde{N}} n_k \frac{\partial E_k}{\partial \boldsymbol{u}_i}(\tilde{\boldsymbol{u}}) \right] \cdot \tilde{\boldsymbol{v}}_i \\ \tilde{Q}(\tilde{\boldsymbol{u}}) &= -\sum_{i=1}^{M} \frac{\partial E_i}{\partial \boldsymbol{u}_{,i}}(\tilde{\boldsymbol{u}}) \cdot \boldsymbol{n} \end{aligned} \tag{38}$$

Note that $\tilde{B}$ is computed using the $\tilde{N}$ representative atoms in the partition $\tilde{\mathcal{P}}_h$. We emphasize here that the approximation $\tilde{\boldsymbol{p}}$ of $\boldsymbol{p}$ involves the same types of errors as in $\boldsymbol{u}_0$, but that it also strongly depends on the accuracy of the computed solution $\boldsymbol{u}_0$.

We now define the error estimator with respect to the quantity of interest, Q, as the computable quantity

$$\eta = \tilde{\mathcal{R}}(\tilde{\boldsymbol{\pi}}\boldsymbol{u}_0; \tilde{\boldsymbol{p}}) = \sum_{i=1}^{\tilde{N}_a} \tilde{\boldsymbol{r}}_i(\tilde{\boldsymbol{\pi}}\boldsymbol{u}_0) \cdot \tilde{\boldsymbol{p}}_i \tag{39}$$

and we show in the next section that η is a reasonable estimate of the error $\mathcal{E} = Q(\boldsymbol{u}) - Q_0(\boldsymbol{u}_0) = Q(\boldsymbol{u}) - Q(\boldsymbol{\pi}\boldsymbol{u}_0)$. Finally, the finite element partition $\tilde{\mathcal{P}}_h$, or enriched mesh, for the calculation of the dual approximation $\tilde{p}$ and the residual $\tilde{\boldsymbol{r}}$ is constructed using the adaptive technique described in Remark 3 using a smaller tolerance than 0.075. In order to assess the quality of the error estimate, we will use the effectivity index defined as the ratio $\zeta = \eta/\mathcal{E}$.

3.4 Numerical experiments. We perform here a few numerical experiments using the same setting as in Section 2.3 in order to study the performance of the error estimator. We first investigate the influence of approximating the dual solution in the enriched space $\tilde{V}$ rather than in the space V_0. Close-up views of the meshes (QCM and enriched meshes) corresponding to these spaces are shown in Fig. 6. As expected, the error estimator performs very poorly when the dual solution is approximated on the QCM mesh. This is clearly indicated in Fig. 7 where it is shown that the error estimator detects very little error at all load steps. By contrast, the error estimator provides reasonable estimates when the enriched space $\tilde{V}$ is used for the approximation of the dual solution, as shown in Fig. 8. The effectivity indices remain mostly close to unity, except maybe in the region of dislocation nucleation where strong nonlinear behavior

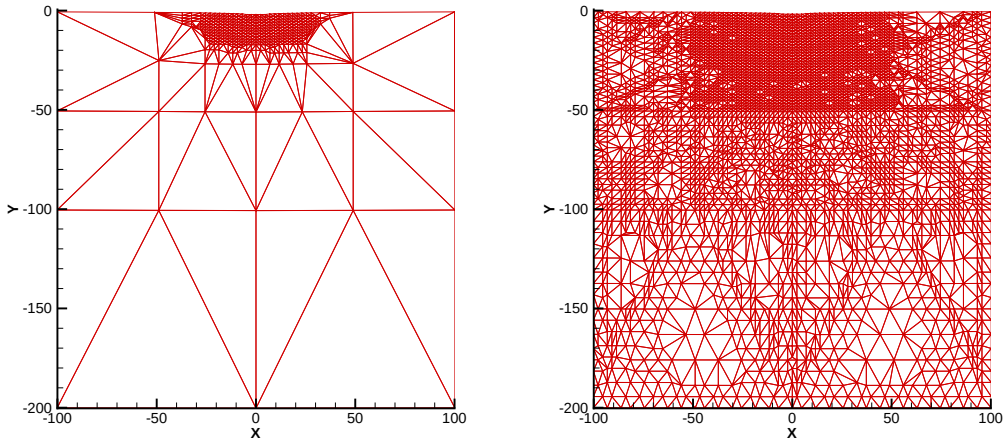

Fig. 6. QCM mesh (left) and enriched mesh (right) at load step 9. The QCM mesh has 432 atoms while the enriched mesh contains 10887.

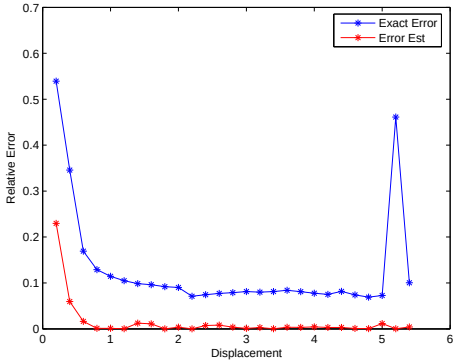

Fig. 7. The (relative) exact error and the error estimate on the QCM mesh without enrichment.

occurs. Indeed, recall that the QC solution dislocates one load step early. In other words, the primal solution $\boldsymbol{u}_0$ contains large errors that certainly pollute the approximation of the dual solution at that particular load step. We actually show in Fig. 9 the dual solutions $\boldsymbol{p}$ and $\boldsymbol{p}_0$ computed using the base model and QCM, respectively, and $\boldsymbol{p}$ exhibits many more details than $\boldsymbol{p}_0$, notably in the region away from the indenter near the slip plane.

4 Adaptivity

We propose here a simple adaptive strategy to control the error in the quantity of interest within some prescribed tolerance δ_{tol}. Our approach is different from the one used in the QCM code, but was made to fit the data structure available

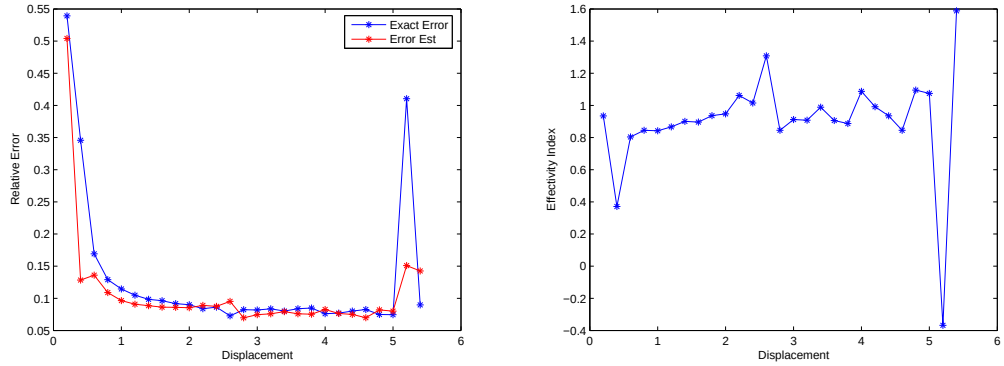

Fig. 8. The relative error (left) and the effectivity indices (right) are shown comparing the error estimator to the exact error for the enriched QCM mesh.

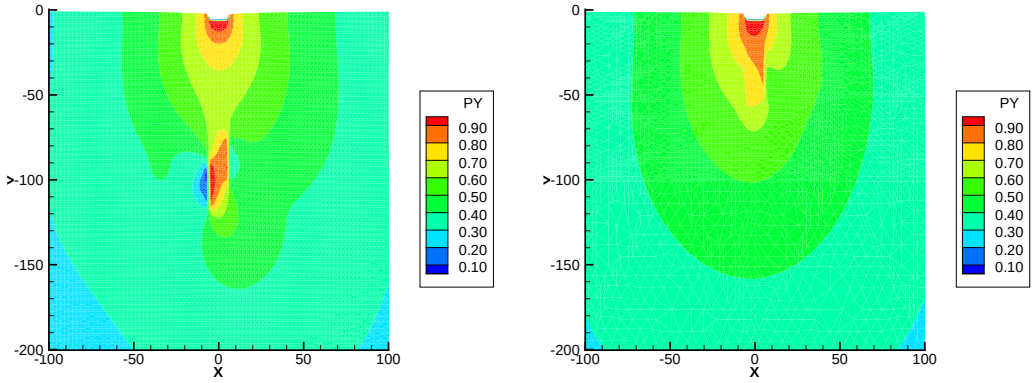

Fig. 9. The dual solution of the base model (left) and the QCM (right) at the beginning of load step 27.

in the code.

4.1 Adaptive strategy. For the purpose of spatial adaptation with respect to the quantity of interest, it is first necessary to decompose the error estimate η into local contributions that could be employed for the development of refinement indicators. Due to the structure of the code, we have adopted an approach in which the local contributions are defined per element such that:

$$\eta = \sum_{K=1}^{N_e} \eta_K \tag{40}$$

This is accomplished in practice as follows: for each element K of the partition, one computes the nodal contributions $\eta_i^K = \tilde{\boldsymbol{r}}_i(\tilde{\boldsymbol{\pi}}\boldsymbol{u}_0)\cdot\tilde{\boldsymbol{p}}_i$ of the quantity η, from

which one can calculate an elementwise contribution as:

$$\eta_K(\tilde{\boldsymbol{\pi}}\boldsymbol{u}_0, \tilde{\boldsymbol{p}}) = \frac{3}{|K|N_i^K} \int_{\Omega_K} \sum_{i=1}^{N_d} \eta_i^K \phi_i \, dx, \tag{41}$$

where $|K|$ denotes the area of element K, N_d the number of nodes in K, N_i^K the number of elements sharing node i, and ϕ_i the restrictions to element K of the linear base functions as defined in (9). This decomposition is simple and easily implemented in the QCM code, but is not unique.

The adaptive algorithm, the so-called Goals algorithm [13], proceeds as follows:

(1) Initialize the load step to $s = 0$. Input user-tolerance δ_{tol}.
(2) Go to the next load step, $s = s + 1$.
(3) Solve the primal and dual problems as described in Sections 2.2 and 3.2, respectively.
(4) Compute the error estimate as discussed in Section 3.3.
(5) If $|\eta| < \delta_{tol}|Q(\boldsymbol{u}_0)|$, go to step (2). Otherwise, mark those elements that satisfy $|\eta_K(\tilde{\boldsymbol{\pi}}\boldsymbol{u}_0, \tilde{\boldsymbol{p}})| > \gamma \max_K |\eta_K(\tilde{\boldsymbol{\pi}}\boldsymbol{u}_0, \tilde{\boldsymbol{p}})|$, where γ is a user-supplied number between 0 and 1.
(6) Refine flagged elements and go to step (3).

Note that our adaptive algorithm slightly differs from QCM in the sense that, in the QCM, the elements are flagged for refinement if the elemental contributions are below some user-specified number γ_{QC} and that the adaptive process within each load step eventually ends when no more elements are flagged for refinement.

4.2 Numerical examples. In the following examples, we choose $\delta_{tol} = 0.05$ (the solution is controlled so that the relative error is always less than five percent) and $\gamma = 0.25$. In Fig. 10, we show the adapted meshes obtained using the QCM and the Goals algorithm once dislocations have nucleated. As can be seen, the Goals mesh includes many more atoms near the indenter. Fig. 11 shows the evolution of the number of atoms (degrees of freedom) for both methods. It is interesting to see that the Goals algorithm adds many repatoms at the beginning of the simulation while QCM essentially refines at the dislocation nucleation.

Force-displacement curves are shown in Fig. 12. We observe that the Goals algorithm is able to control the error within the specified tolerance and provides a solution that predicts the dislocation nucleation just as the base model solution does, but at a much lower computational cost. Relative errors and effectivity indices are plotted in Fig. 13, demonstrating the effectiveness of

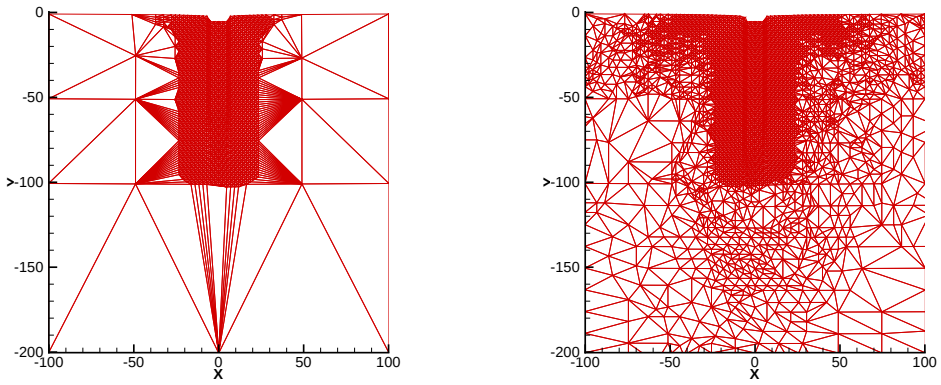

Fig. 10. QCM (left) and Goals (right) mesh at load step 27. The number of atoms in the QCM and Goals meshes are 1629 and 3452, respectively.

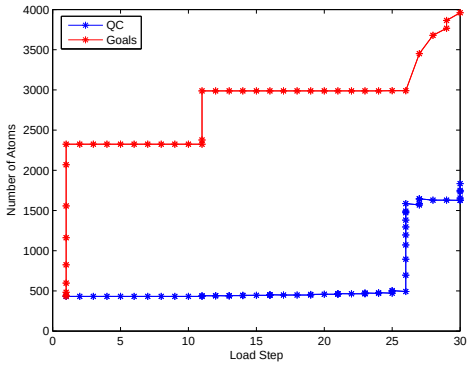

Fig. 11. Comparison of the evolution of QCM mesh and Goals mesh.

our error estimator. Finally, we show in Fig. 14 the dual solutions obtained using the base model, the QCM, and the Goals algorithm. Again, this result shows that the dual solutions for the base model and the Goals algorithm are virtually indistinguishable while the solution of the QCM is very different.

5 Conclusions

In the present work, we have extended the methodology of goal-oriented error estimation and adaptivity to molecular statics using approximate solutions produced by the quasicontinuum method (QCM). Estimates of the error in the QC approximations with respect to quantities of interest are derived and are used as a basis for the development of a Goals algorithm. The theoretical results were applied to a sample nanoindentation problem and it was found that the Goals methodology provides reliable error estimates and successfully

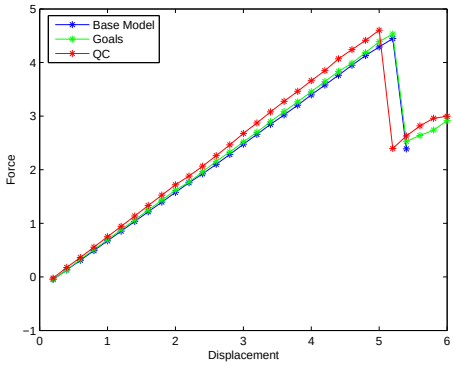

Fig. 12. Force-displacement curves computed from the base model solution, the QC solution, and the Goals solution.

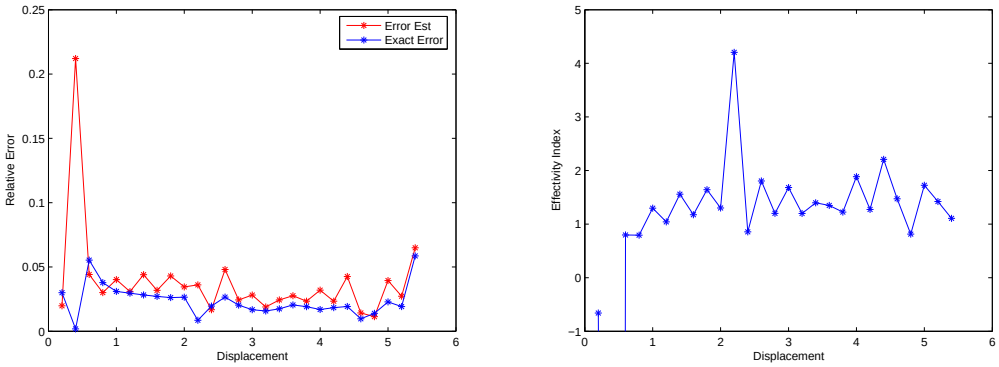

Fig. 13. Relative error (left) and effectivity indices (right).

controls the prediction of the force acting on the indenter. The results were consistently verified using a highly resolved solution of the nanoindentation problem.

Acknowledgments. Paul T. Bauman gratefully acknowledges the Department of Energy Computational Science Graduate Fellowship for financial support. Support of this work by ONR under Contract No. N00014-99-1-0124 is gratefully acknowledged.

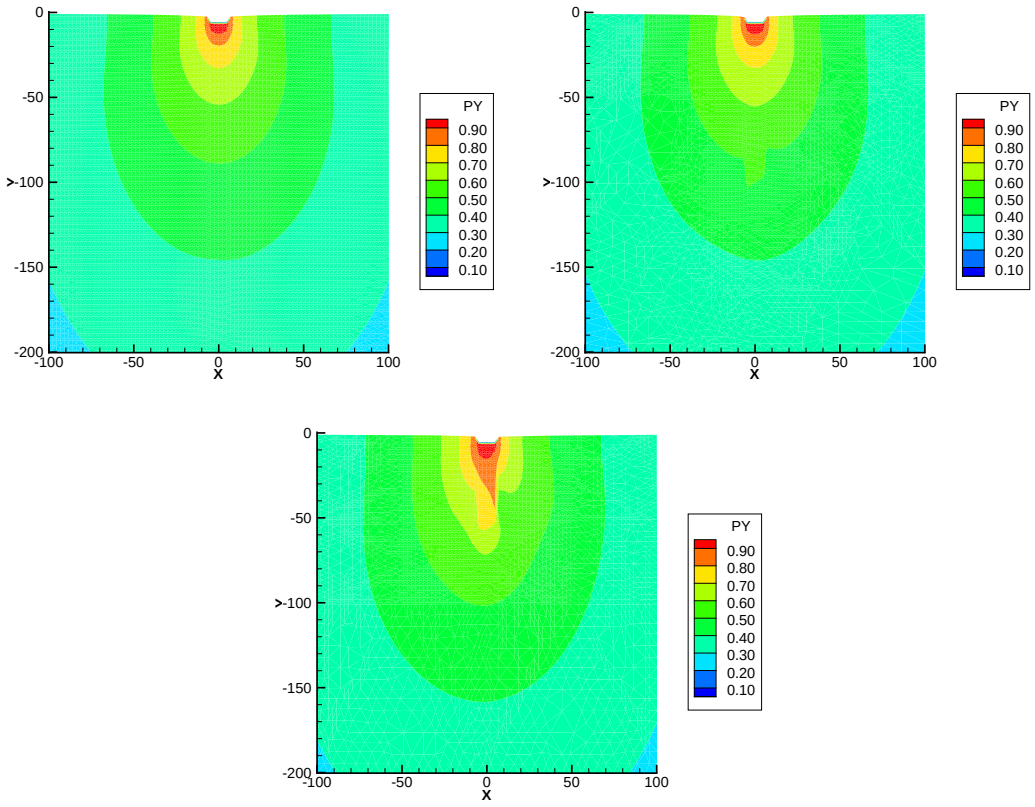

Fig. 14. Comparison of the dual solution for the base model (top left), the Goals algorithm (top right), and the QCM (bottom) at the end of load step 27.

References

[1] J. Q. Broughton, F. F. Abraham, N. Bernstein, and E. Kaxiras. Concurrent coupling of length scales: Methodology and application. *Physical Review B*, 60(4):2391–2403, 1999.

[2] W. A. Curtin and R. E. Miller. Atomistic/continuum coupling in computational materials science. *Modelling Simul. Mater. Sci. Eng.*, 11:R33–R68, 2003.

[3] M. S. Daw and M. I. Baskes. Semiempirical, quantum mechanical calculation of hydrogen embrittlement in metals. *Physical Review Letters*, 50(17):1285–1288, 1983.

[4] M. S. Daw and M. I. Baskes. Embedded-atom method: Derivation and applications to impurities, surfaces, and other defects in metals. *Physical Review B*, 29(12):6443–6453, 1984.

[5] F. Ercolessi and J. Adams. Interatomic potentials from 1st-principles

calculations – the force-matching method. *Europhysics Letters*, 26:583–588, 1993.

[6] S. M. Foiles, M. I. Baskes, and M. S. Daw. Embedded-atom-method functions for fcc metals Cu, Ag, Au, Ni, Pd, Pt, and their alloys. *Physical Review B*, 33(12):7983–7991, 1986.

[7] G. Friesecke and F. Theil. Validity and failure of the Cauchy-Born hypothesis in a two-dimensional mass-spring lattice. *J. Nonlinear Sci.*, 12:445–478, 2002.

[8] W. K. Liu, E. G. Karpov, S. Zhang, and H. S. Park. An introduction to computational nanomechanics and materials. *Comput. Methods Appl. Mech. Engng.*, 193:1529–1578, 2004.

[9] R. E. Miller and E. B. Tadmor. The quasicontinuum method: Overview, applications, and current directions. *Journal of Computer-Aided Design*, 9:203–239, 2002.

[10] R. E. Miller and E. B. Tadmor. *QC Tutorial Guide Version 1.1*, May 2004. Available at www.qcmethod.com.

[11] J. T. Oden and S. Prudhomme. Estimation of modeling error in computational mechanics. *Journal of Computational Physics*, 182:496–515, 2002.

[12] J. T. Oden, S. Prudhomme, and P. Bauman. On the extension of goal-oriented error estimation and hierarchical modeling to discrete lattice models. *Comput. Methods Appl. Mech. Engrg.*, 194:3668–3688, 2005.

[13] J. T. Oden, S. Prudhomme, A. Romkes, and P. Bauman. Multi-scale modeling of physical phenomena: Adaptive control of models. ICES Report 05-20, The University of Texas at Austin, 2005. Submitted to SIAM Journal on Scientific Computing.

[14] J. T. Oden and K. Vemaganti. Estimation of local modeling error and goal-oriented modeling of heterogeneous materials 1. Error estimates and adaptive algorithms. *Journal of Computational Physics*, 164:22–47, 2000.

[15] R. Phillips, D. Rodney, V. Shenoy, E. B. Tadmor, and M. Ortiz. Hierarchical models of plasticity: dislocation nucleation and interaction. *Modeling Simul. Mater. Sci. Eng.*, 7:769–780, 1999.

[16] A. Romkes and J. T. Oden. Adaptive modeling of wave propagation in heterogeneous elastic solids. *Comput. Methods Appl. Mech. Engng.*, 193:539–559, 2004.

[17] V. B. Shenoy, R. Miller, E. B. Tadmor, D. Rodney, R. Phillips, and M. Ortiz. An adaptive finite element approach to atomic-scale mechanics — the quasicontinuum method. *Journal of the Mechanics and Physics of Solids*, 47:611–642, 1999.

[18] E. B. Tadmor. *The Quasicontinuum Method*. PhD thesis, Brown University, 1996.

[19] E. B. Tadmor, R. Miller, R. Phillips, and M. Ortiz. Nanoindentation and incipient plasticity. *J. Mater. Res.*, 14:2233–2250, 1999.

[20] E. B. Tadmor, M. Ortiz, and R. Phillips. Quasicontinuum analysis of defects in solids. *Phil. Mag. A*, 73(6):1529–1563, 1996.

[21] O. C. Zienkiewicz and J. Z. Zhu. A simple error estimator and adaptive procedure for practical engineering analysis. *Int. J. Numer. Methods Engrg.*, 24:337–357, 1987.